Macrostructural Changes in Thermally Treated Viscose Fibers Due to Cold Drawing Process

I. M. FOUDA, H. M. SHABANA

Department of Physics, University of Mansoura, Mansoura 35516, Egypt

Received 4 May 2000; accepted 2 December 2000

ABSTRACT: The molecular orientation of thermally treated viscose (rayon) fibers was investigated by two techniques. The mechanical parameters, which were obtained by a micro-stress–strain device in conjunction with an interference microscope, and structural parameters, which gave the optical properties, of boiled viscose fibers for different intervals of time and cold drawn at room temperature were calculated. The changes in the stress and draw ratios were evaluated to obtain the shrinkage factor, uniaxial tension, and true stress and orientation factors $\langle P2(\cos\theta)\rangle$ and $\langle P4(\cos\theta)\rangle$. The functions $f_2(\theta)$, $f_4(\theta)$, and $f_6(\theta)$ were also calculated. The dielectric constant, dielectric susceptibility, number of moles in physical network chains between entanglements in the semicrystalline phase per unit volume, surface reflectivity, segment anisotropy, number of chains between crosslinks per unit volume, and number of crystals per unit volume were among the evaluated parameters. An empirical formula was suggested to correlate the changes in the evaluated parameters with different draw ratios, and its constants were determined. The study demonstrated changes in the molecular orientation factors and the evaluated macrostructural parameters as a result of applied stress and the boiling effect. © 2001 John Wiley & Sons, Inc. J Appl Polym Sci 82: 2387–2398, 2001

Key words: viscose fibers; interferometry; orientation; mechanical; dielectric; shrinkage

INTRODUCTION

Mechanical deformation on polymers can produce changes in the chain segments. The drawing process gives rise to a preferred orientation of the molecular chain axis, which can be described by orientation distribution functions.[1–5] Statton et al.[3] proposed that shrinkage should be attributed to the refolding of chains pulled out in the drawing process.

The drawing of macromolecular samples represents one of the most effective methods for changing the orientation of polymer chains. In most instances, the chain orients parallel to the draw direction. A full description of the drawing process is complicated by the large variety of possible starting materials that are usually not fully characterized. A sample may range from fully amorphous to fully crystalline in the degree of crystallization.[6]

Studying fibrous materials by interferometry to attain the principal optical parameters such as the refractive indices and birefringence is extensively discussed by many authors.[7–10] These parameters contribute to characterizing the structure of such materials for human use. Good thermal stability is an attractive characteristic that makes fibers more suitable for several applica-

Correspondence to: I. M. Fouda (sinfac@mum.mans.eun.eg).

Journal of Applied Polymer Science, Vol. 82, 2387–2398 (2001)

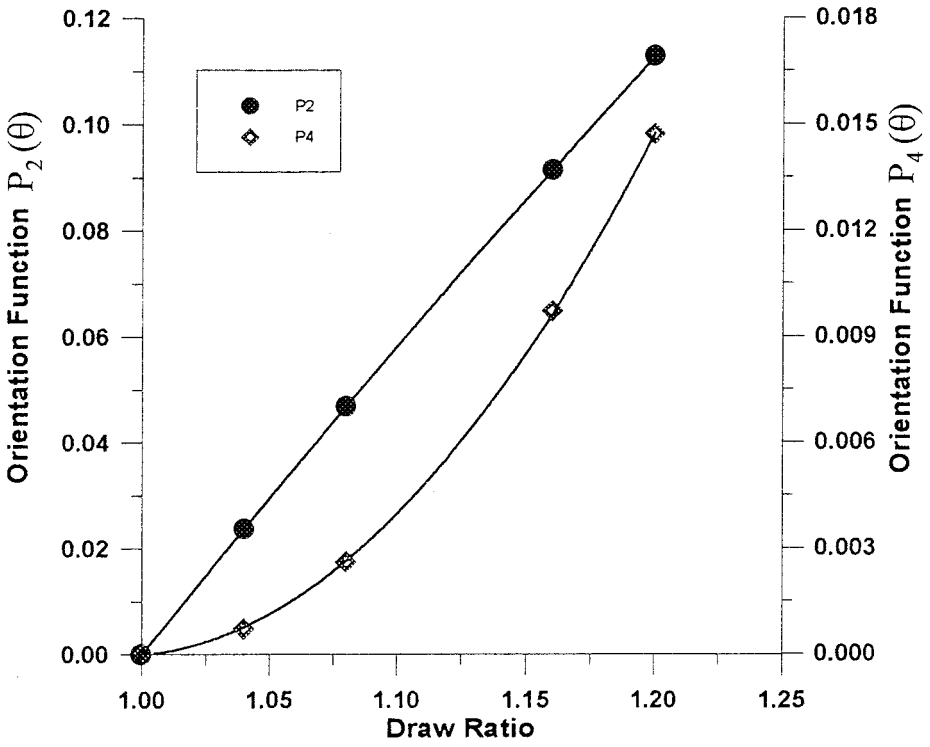

Figure 1 The parameters $P_2(\theta)$ and $P_4(\theta)$ as a function of the draw ratio.

tions. Improving the thermal resistance of fibers by suitable treatments is a new approach in research that is designed to elucidate fiber structural order to produce materials with new physical properties and hence expand their utilization under different conditions.[11–13]

The present work investigated the molecular orientation parameters produced in viscose fibers (viscose rayon filament, Misr Co. of Artificial Silk) under different conditions using a double-beam interference microscope connected to a stress–strain device. The variations in the refractive indices and birefringence with different stresses were used to calculate the shrinkage stress, true stress, and uniaxial tension. Various orientation functions, orientation angles, and other structural parameters were also calculated. In addition, the dielectric constant, dielectric susceptibility, and surface reflectivity were determined at different stresses and different intervals of boiling times.

THEORETICAL

Two-Beam Interferometry

The two-beam interference technique is used extensively for determining optical parameters such as the refractive indices, the light vibrating along and across the fiber axis, and the birefringence. These parameters and others were determined by using the following equation[8–10]:

$$n^{\parallel} = n_L + (F^{\parallel}D/A)(\lambda/h) \quad (1)$$

and an analogous equation for $n^{\parallel}$, where n_L is the liquid refractive index, h is the interfringe spacing, D is the draw ratio, A is the cross-sectional area of the undrawn sample, A/D is the cross-sectional area of the drawn sample, $F^{\parallel}$ is the area under the fringe shift, λ is the wavelength of the source used, and $n^{\parallel}$ and $n^{\perp}$ are the respective refractive indices of the fiber when the light is vibrating along and across the axis of the fiber. The above optical parameters were used in the present study to focuses attention on essential industrial parameters such as the dielectric, orientation functions, shrinkage, cohesive energy density (CED), and so forth.

Mechanical Parameters

Shrinkage Stress

The shrinkage stress S is related to the draw ratio by the following relation[14]:

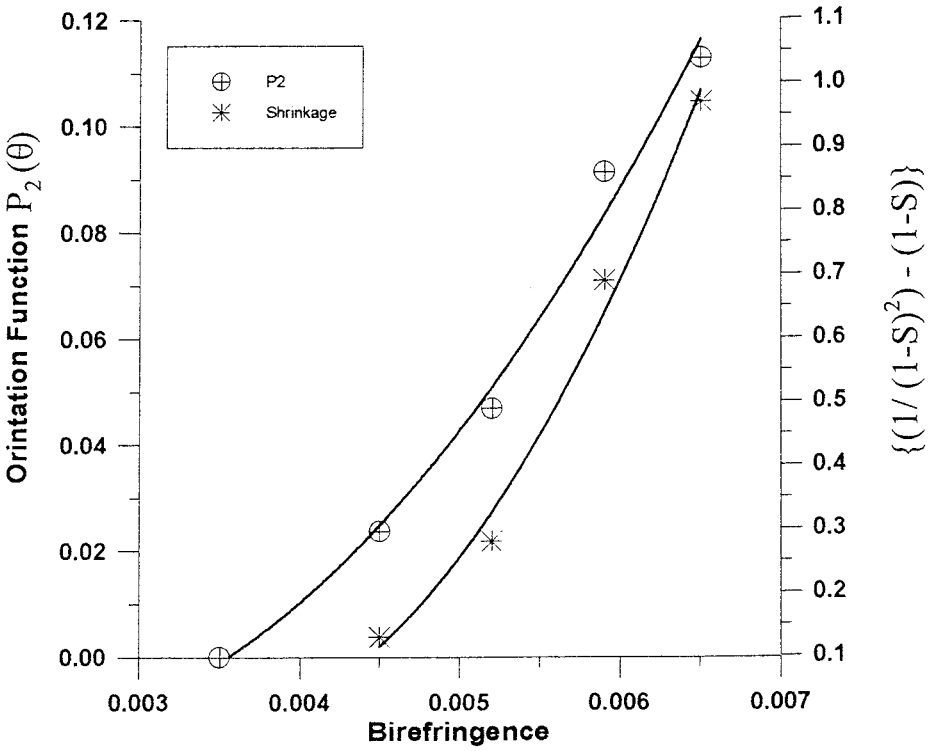

Figure 2 The relationships between the shrinkage factor $\{[1/(1-S)^2] - (1-S)\}$, the mechanical orientation $P_2(\theta)$, and the birefringence.

$$S = (D - 1)D \tag{2}$$

where D is the draw ratio of the final fiber length/starting length. If the shrinkage force can be measured, the stress optical coefficient can be used to calculate the number of monomer units per link.

The uniaxial tension can be estimated from the following equation:

$$\sigma = G(D^2 - D^{-1}) \tag{3a}$$

where G is the elastic shear modulus. The true stress is given by

$$\sigma' = G(D - D^{-2}) \tag{3b}$$

The value of the bulk modulus B is related to the CED, which represents the energy theoretically required to move a detached segment into the vapor phase. This in turn is related to the square of the solubility parameter

$$(1 - 2\mu = E/3B = \beta E/3) \tag{4a}$$

$$B = 8.04(\text{CED}) = 8.04\delta^2 \tag{4b}$$

where μ is Poisson's ratio and β is the compressibility. The factor 8.04 arises from Lennard–Jones considerations.[15]

Mechanical Orientation

On the aggregate model the low strain mechanical anisotropy is related to the orientation functions $\langle P_2(\cos\theta)\rangle$ and $\langle P_4(\cos\theta)\rangle$. These functions provide some understanding of the mechanism of deformation. By considering the network as freely jointed chains of identical links called random links, $\langle P_2(\cos\theta)\rangle$ is given by[16,17]

$$\langle P_2(\theta)\rangle = \frac{1}{2}\left[\frac{2 + U^2}{1 - U^2} - \frac{3U\cos^{-1}U}{(1 - U^2)^{3/2}}\right] \tag{5}$$

where $U = D^{-3/2}$. Using the Treloar[18] expression for the inverse Langevin function we can find $\langle P_2(\cos\theta)\rangle$ as follows:

$$\langle P_4(\theta)\rangle = \frac{1}{8}\left\{\begin{array}{c}\dfrac{35}{(1 - U^2)^2}\left[1 + \dfrac{U^2}{2} - \dfrac{3U\cos^{-1}U}{2(1 - U^2)^{1/2}}\right] \\ -\dfrac{30}{(1 - U^2)}\left[1 - \dfrac{U\cos^{-1}U}{(1 - U^2)^{1/2}}\right] + 3\end{array}\right\} \tag{6}$$

Table I Draw Ratios, Birefringence, Uniaxial Tension, True Stress, Optical Orientation Functions, and Number of Moles

D	Δn_a ($\times 10^{-3}$)	σ ($\times 10^{10}$)	σ' ($\times 10^{10}$)	$f_2(\theta)$	$f_4(\theta)$	$f_6(\theta)$	m ($\times 10^{-4}$ mol/cm^3)
			Unboiled Sample				
1.00	3.5	—	—	0.0636	−0.416	4.255	—
1.04	4.5	3.58	3.44	0.0818	−0.421	4.440	1.21
1.08	5.2	5.82	5.39	0.0945	−0.424	4.573	1.01
1.16	5.9	8.19	7.11	0.1073	−0.426	4.709	0.74
1.20	6.5	10.06	8.49	0.1182	−0.427	4.828	0.74
			Sample Boiled for 15 min				
1.00	4.0	—	—	0.0727	−0.419	4.347	—
1.04	4.7	2.76	2.65	0.0855	−0.422	4.478	0.94
1.08	5.5	3.63	3.36	0.1000	−0.425	4.631	0.63
1.16	6.2	4.78	4.15	0.1127	−0.427	4.768	0.43
1.20	6.6	5.87	4.94	0.1200	−0.428	4.848	0.43
			Sample Boiled for 30 min				
1.00	4.3	—	—	0.0782	−0.420	4.403	—
1.04	5.1	2.76	2.65	0.0927	−0.424	4.554	0.94
1.08	6.2	4.36	4.04	0.1127	−0.427	4.768	0.75
1.16	7.0	7.99	6.94	0.1273	−0.428	4.929	0.72
1.20	7.3	9.66	8.13	0.1327	−0.428	4.990	0.71
			Sample Boiled for 60 min				
1.00	4.5	—	—	0.0818	−0.421	4.440	—
1.04	5.3	3.58	3.44	0.0964	−0.424	4.592	1.21
1.08	6.3	5.82	5.39	0.1145	−0.427	4.788	1.01
1.16	6.7	6.69	5.81	0.1218	−0.428	4.868	0.60
1.20	7.1	8.04	6.77	0.1291	−0.428	4.949	0.60

Hermans Orientation Functions

Hermans represented the orientation function $f(\theta)$ by a series of spherical harmonics (Fourier series) as follows[17,19]:

$$f(\theta) = \sum_{n=0}^{\infty} \left(n + \frac{1}{2}\right) \langle f_n \rangle f_n(\theta) \tag{7}$$

where the odd components are all zero and the first three even components are given by

$$f_2(\theta) = \frac{1}{2}(3\cos^2\theta - 1) \tag{8a}$$

$$f_4(\theta) = \frac{1}{8}(35\cos^4\theta - 30\cos^2\theta + 3) \tag{8b}$$

$$f_6(\theta) = \frac{1}{6}(231\cos^6\theta - 15\cos^4\theta + 105\cos^2\theta - 5) \tag{8c}$$

The parameters $\langle f_n \rangle$ are the average values (amplitudes). A sample with an orientation function may be considered to consist of perfectly aligned molecules of the mass fraction f and randomly oriented molecules of the mass fraction $(1 - f)$, where f is proportional to the birefringence (Δn) as follows:

$$f_2 = \frac{\Delta n_a}{\Delta n_{\max}} \tag{9}$$

where $\Delta n_{\max}$ is the maximum birefringence. This value for viscose was previously[20] determined to be 0.055.

Determination of Dielectric Constant and Dielectric Susceptibility

The dielectric constant is given by the following relation as explained elsewhere[21]:

$$\varepsilon = \frac{1 + 2(4\pi N\bar{\alpha}/3)}{1 - (4\pi N\bar{\alpha}/3)} \tag{10}$$

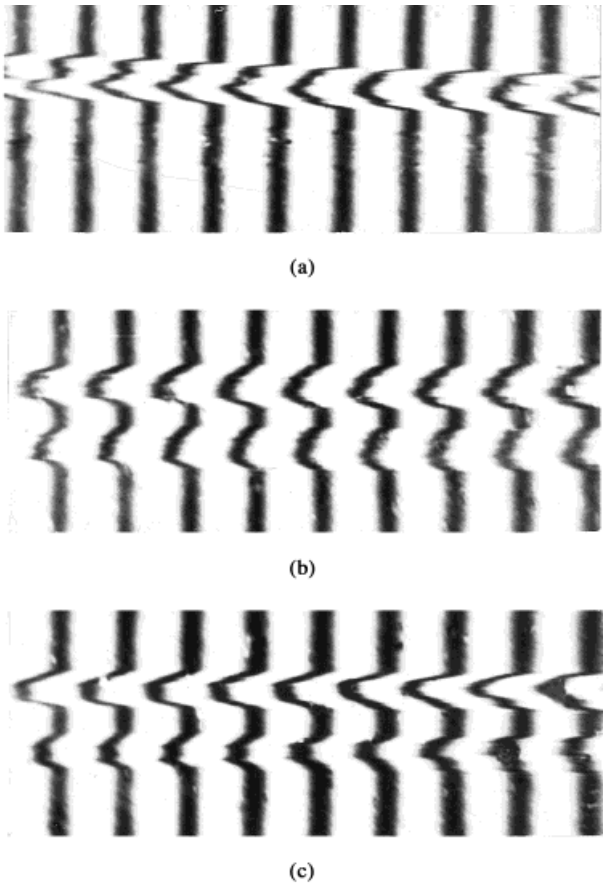

Figure 3 Microinterferograms of the two-beam interferometry at a draw ratio of 1 and boiling times of (a) 0, (b) 15, and (c) 60 min.

where $\bar{\alpha}$ is regarded as the mean polarizability of a monomer unit and N is the number of molecules per unit volume. The dielectric susceptibility η is related to ϵ by the following well-known equation[21]:

$$\eta = \frac{\varepsilon - 1}{4\pi} \tag{11}$$

The number of moles m in physical network chains between entanglements in the semicrystalline phase per unit volume is related to the applied stress σ by the following equation[22]:

$$\sigma = mRT(D - D^{-2}) \tag{12}$$

where R is the gas constant and T is the absolute temperature.

Calculation of Surface Reflectivity, Segment Anisotropy, and Number of Chains Per Unit Volume

The surface reflectivity of a polymer for light at normal incidence can be estimated from Fresnel equations[23] and a knowledge of the mean refractive index $\bar{n}$. Thus, the percentage of reflection R' (in air) is given by

$$R' = \left(\frac{\bar{n} - 1}{\bar{n} + 1}\right)^2 \times 100 \tag{13}$$

The stress optical coefficient C_s, which equals $\Delta n/\sigma$, is used to determine the segment anisotropy γ_s from the following equation[24]:

$$\gamma_s = 90\varepsilon_0 KTC_s \frac{\bar{n}}{(\bar{n}^2 + 2)^2} \tag{14}$$

where K is the Boltzmann constant. The N' at absolute temperature is determined from the following relation[24]:

$$N' = \frac{90\varepsilon_0 \Delta n}{\gamma_s} \frac{\bar{n}}{(\bar{n}^2 + 2)^2} \frac{1}{(D^2 - D^{-1})} \tag{15}$$

where ϵ_o is the permittivity, which equals 8.85 $\times 10^{-12}$ F m^{-1} (m^{-3} kg^{-1} s^4 A^2).

Birefringence of Partially Crystalline Polymers

The birefringence of partially crystalline polymers[24] was found with three equations. The average orientation angle on the uniaxial stretching extension ratio D is given by

$$\langle \cos^2\theta_c \rangle = \frac{D^3}{D^3 - 1}\left[1 - \frac{\tan^{-1}(D^3 - 1)^{1/2}}{(D^3 - 1)^{1/2}}\right] \tag{16}$$

If there are Y crystals per unit volume, and these have polarizabilities b_c along c axis and $b_b = b_a$ perpendicular to it, then the crystal contribution to the birefringence of the medium is given by

$$Y = 18\varepsilon_o \Delta n \frac{\bar{n}}{(\bar{n}^2 + 2)^2} \frac{1}{(b_b - b_a)\langle P_2(\cos\theta_c)\rangle} \tag{17}$$

where $P_2(\cos\theta_c) = 1/2(3\cos^2\theta_c - 1)$, which is the orientation function of the chain, and $(b_b - b_a)$, which is the optical configuration parameter, equals

$$b_b - b_a = \frac{(45KTC_s/2\pi)\bar{n}}{(\bar{n}^2 + 2)^2}$$

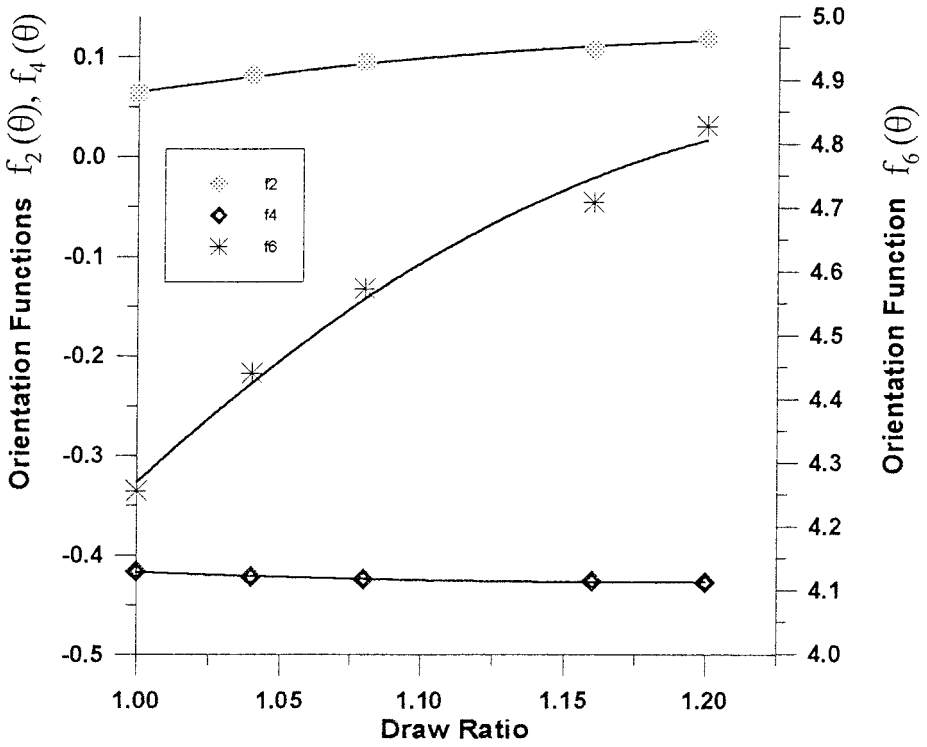

Figure 4 The relationships between the optical orientation functions $f_2(\theta)$, $f_4(\theta)$, and $f_6(\theta)$ and the draw ratios for the unboiled sample.

EXPERIMENTAL

Investigating the mechanical and structural changes in viscose fibers (manufactured in Egypt by Misr rayon co. of artificial silk) and their correlation to their optical properties was done using a micro-stress–strain device attached to a Pluta polarizing interference microscope.[25,26] The untreated samples (glass-transition temperature of 45.9°C and crystallinity index of 0.22) were boiled for different intervals of time. The microstrain device was used to measure stress and strain. It was connected to the two-beam polarizing interference Pluta microscope to measure the refractive indices for the two principal vibration directions and the birefringence values as a function of the stress, strain, and draw ratio of the viscose fibers.

The previously obtained data[10] for the $n^{\parallel}$, $n^{\perp}$, Δn, and stress were used in the present work to calculate the mechanical parameters such as the shrinkage stress, uniaxial tension, true stress, and orientation factors $P_2(\theta)$ and $P_4(\theta)$, and structural parameters such as the orientation factors $f_2(\theta)$, $f_4(\theta)$, and $f_6(\theta)$ and their relation to the optical parameters, R, ϵ, and η, and other parameters.

Calculation of Mechanical Parameters

The shrinkage stress was calculated from eq. (1). The mechanical orientation factors given by Stein[16] [$P_2(\theta)$ and $P_4(\theta)$] were calculated and drawn as a function of the draw ratio as in Figure 1, where both parameters increase as the draw ratios increase. Because $P_2(\theta)$ and $P_4(\theta)$ are mechanically dependent, they are unaffected by boiling. It is notable that the $P_4(\theta)$ values are always comparatively small. The shrinkage factor $\{[1/(1 - S)^2] - (1 - S)\}$ and mechanical orientation $P_2(\theta)$ and their relationships with the birefringence are given in Figure 2, where both parameters increase as the birefringence increases. The first explains the use of the factor $\{[1/(1 - S)^2] - (1 - S)\}$ as the ordinate in this figure, whereas the second describes the deformation scheme that is based on the idea that the polymer consists of an aggregate of transversely isotropic units whose symmetry axes rotate on drawing in the same manner as lines joining pairs of points in the bulk material.[27] The uniaxial tension and true stress were calculated using eqs. (2) and (3). The obtained results are given in Table I; they increase with increasing the applied stress and boiling effect.

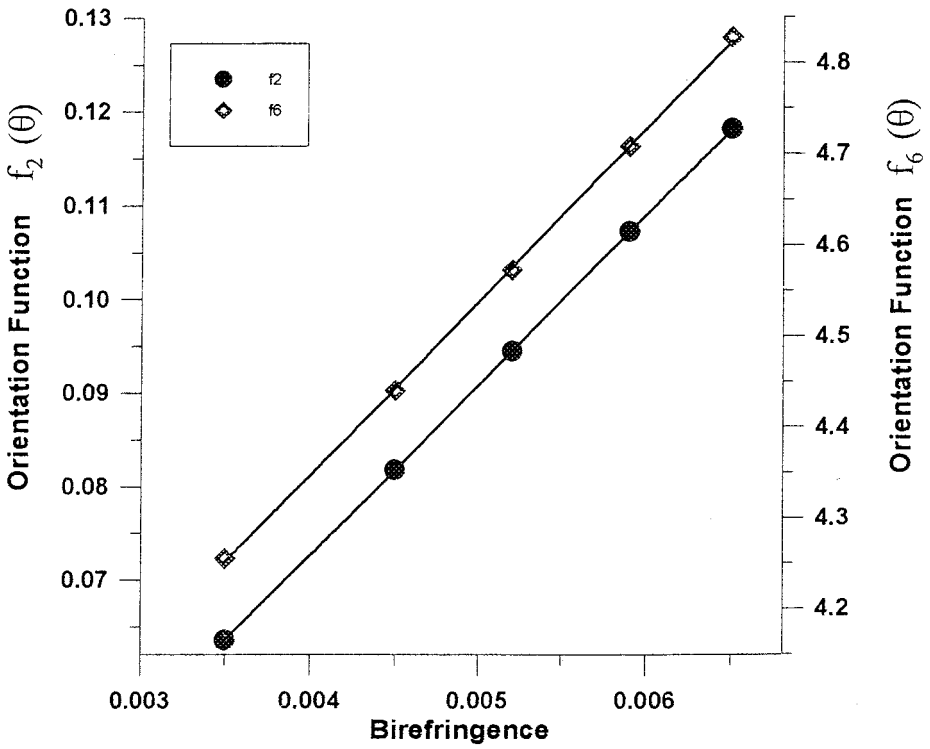

Figure 5 The optical orientation factors $f_2(\theta)$ and $f_6(\theta)$ as a function of the optical birefringence.

Birefringence–Strain Relationship

Following the well-known Mooney–Rivilin equation, the birefringence–strain relation is given as follows[24]:

$$\Delta n = (D - D^{-2})\left(A_1 + \frac{A_2}{D}\right) \tag{18}$$

A plot of $\Delta n/(D - D^{-2})$ against the reciprocal elongation D^{-1} gives a straight line whose slope is A_2 and intercept with the ordinate is A_1. The values obtained for A_1 and A_2 wer -0.151 and 0.193, respectively, for the unboiled sample. In general, the A_2/A_1 ratio was approximately similar to C_2/C_1 for the Mooney–Rivilin equation, so the birefringence remained proportional to the stress.[28]

Application of Two-Beam Interferometry

Figure 3(a–c) shows some of the microinterferograms obtained by the two-beam interferometry from the nonduplicated image position. The plane polarized light of 546-nm λ and a liquid of 1.5761 n_L at 31°C were used. The corresponding draw ratio was 1 and the boiling times were 0, 15, and 60 min. At different draw ratios the previously[10] calculated $n^{\parallel}$, $n^{\perp}$, and Δn were used to calculate various parameters. The resultant data for birefringence are given in Table I.

Evaluation of Molecular Orientation

In view of the relevance of the optical orientation functions given by Hermans [$f_2(\theta)$, $f_4(\theta)$, $f_6(\theta)$] to the deformation mechanism, it was interesting to calculate their values as seen in Table I. The optical birefringence gives a direct measure of these parameters on the basis of the aggregate model and the calculated values for these orientation functions are useful in predicting optical and mechanical anisotropy presented in viscose fibers. Figure 4 shows the relationships between the draw ratios and the optical orientation functions $f_2(\theta)$, $f_4(\theta)$, and $f_6(\theta)$ for the unboiled sample. For the samples boiled for 15, 30, and 60 min the same behavior was obtained with some differences as a result of the boiling effect. The optical orientation functions $f_2(\theta)$ and $f_6(\theta)$ were drawn as a function of the birefringence for the unboiled

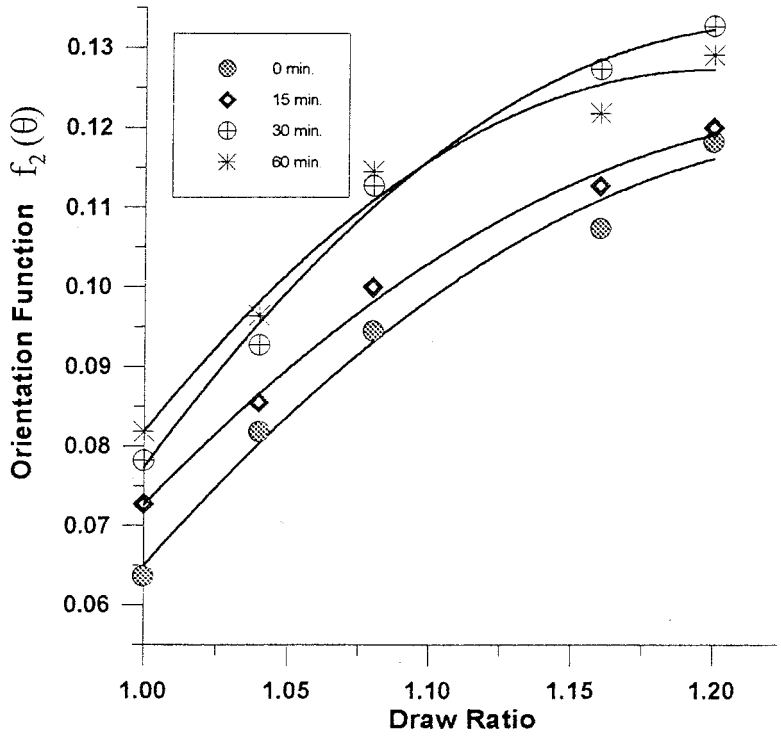

(a)

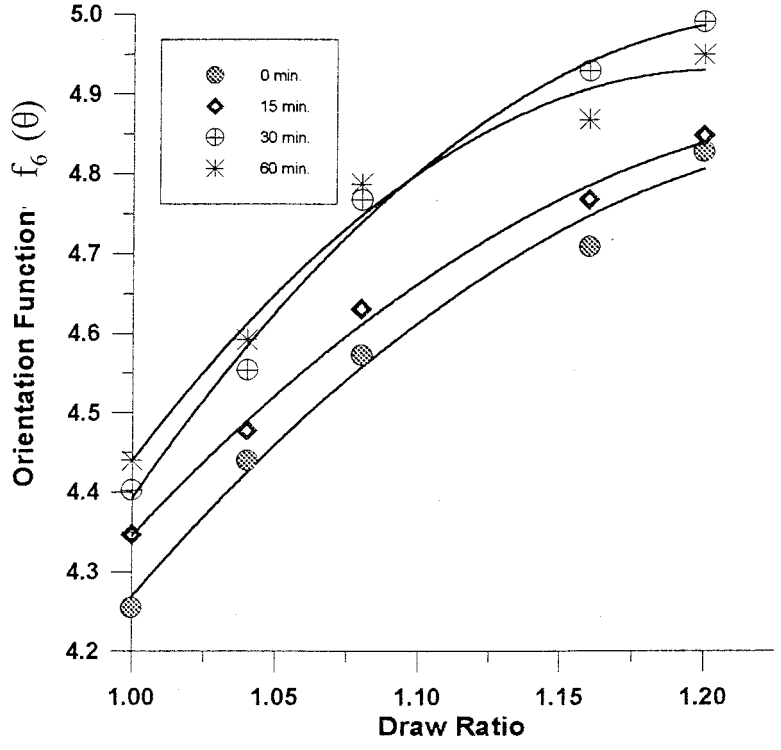

(b)

Figure 6 The optical orientation functions (a) $f_2(\theta)$ and (b) $f_6(\theta)$ as a function of the draw ratios and boiling times.

Table II Draw Ratios, Cohesive Energy Density (CED), Segment Anisotropy, Number of Chains between Crosslinks/Unit Volume, and Number of Crystals/Unit Volume

D	CED ($\times 10^8$)	γ_s ($\times 10^{-43}$ s^4 A^4 kg^{-1})	N' ($\times 10^{32}$)	Y ($\times 10^6$ F mm^{-4})
		Unboiled Sample		
1.00	—	—	—	—
1.04	9.21	0.345	0.702	0.791
1.08	3.68	0.249	0.562	0.641
1.16	1.44	0.205	0.385	0.452
1.20	1.09	0.186	0.371	0.444
		Sample Boiled for 15 min		
1.00	—	—	—	—
1.04	7.06	0.467	0.542	0.610
1.08	2.29	0.422	0.351	0.400
1.16	0.84	0.369	0.225	0.264
1.20	0.63	0.325	0.217	0.259
		Sample Boiled for 30 min		
1.00	—	—	—	—
1.04	7.06	0.507	0.542	0.610
1.08	2.75	0.396	0.421	0.480
1.16	1.41	0.249	0.375	0.441
1.20	1.04	0.218	0.356	0.426
		Sample Boiled for 60 min		
1.00	—	—	—	—
1.04	9.21	0.406	0.702	0.791
1.08	3.68	0.302	0.562	0.641
1.16	1.18	0.285	0.314	0.370
1.20	0.87	0.255	0.297	0.355

sample as in Figure 5. The same behavior was obtained for the boiled samples. The effect of boiling on the orientation functions $f_2(\theta)$ and $f_6(\theta)$ is shown in Figure 6(a,b).

The ϵ and η were determined from eqs. (10) and (11), respectively, and were found to be constant with different boiling times. The ϵ and η results were 2.34 and 0.106, respectively. The m in physical network chains between entanglements in the semicrystalline phase per unit volume and the surface reflectivity were estimated from eqs. (12) and (13), respectively. The values obtained for m are given in Table I; the surface reflectivity was determined to be 4.37%.

In addition, the λ_s, N' of chains between crosslinks per unit volume, and Y of crystals per unit volume were also calculated at different draw ratios and boiling times. The resulting data for these parameters are given in Table II. The N' and Y are plotted against the draw ratio and birefringence in Figure 7(a,b) for the unboiled sample. Similar behavior with slight changes was seen for the samples boiled for different intervals of time. Figure 7(a,b) shows that the N' and Y decreased with increasing draw ratio and birefringence.

The CED was calculated from eq. (17). These CED values are given in Table II. The segment anisotropy and CED decreased as the draw ratio increased, which is shown in Figure 8.

Correlation between Evaluated Parameters and Draw Ratio

An empirical formula was suggested to correlate the change in $f_2(\theta)$, $f_6(\theta)$, σ', δ^2, γ_s, N', and Y with the draw ratio as follows:

$$\ln \frac{f_2(\theta) f_6(\theta) \sigma'}{8.04 \delta^2 \gamma_s N' Y} = XD + Z \tag{19}$$

where X and Z are constants characterizing the proportionality in eq. (19). The values of X and Z were found to be 33.15 and −18.19, respectively.

DISCUSSION

The drawing of a polymer produces reorientation at a macrostructure level whereas thermal processes increase the mobility of the chains and the axial mobility of the microfibrils.[29] In general, both processes change the crystalline and amorphous parts in several kinds of fibers, including viscose, where the crystallized areas give a high modulus of rigidity, elasticity, and ultimate tensile strength to the viscose fibers. The amorphous areas give the flexibility, recovery, elongation, and swelling. Significant variations in the characteristic properties of the investigated fibers were due to reorientation of the molecules and changed the structural behavior due to accumulation of structural phenomena. The change in free volume due to mass redistribution associated with the boiling and drawing conditions affected the obtained parameters.[30]

The mechanical anisotropy for semicrystalline polymers is deformed by cold drawing, because it enables the mechanical factors $P_2(\theta)$ and $P_4(\theta)$ to be calculated as a function of the draw ratio.[31,32] The differences in their values in comparison with those for $f_2(\theta)$ and $f_4(\theta)$ may arise from the fact that the $P_2(\theta)$ and $P_4(\theta)$ factors are only functions of the draw ratio.

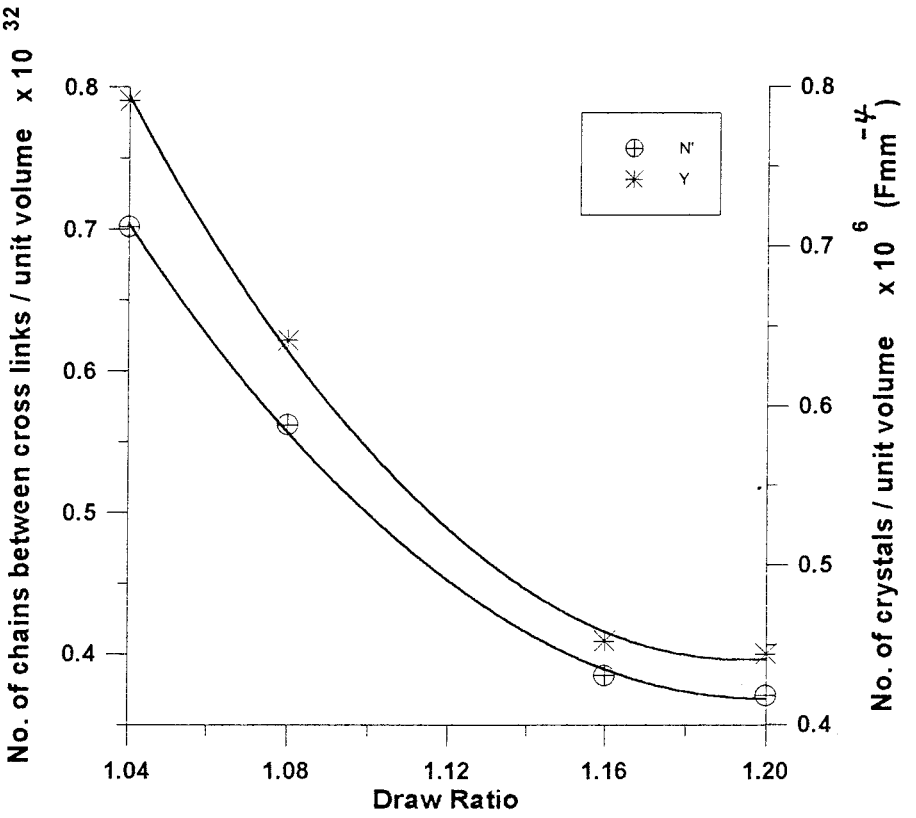

(a)

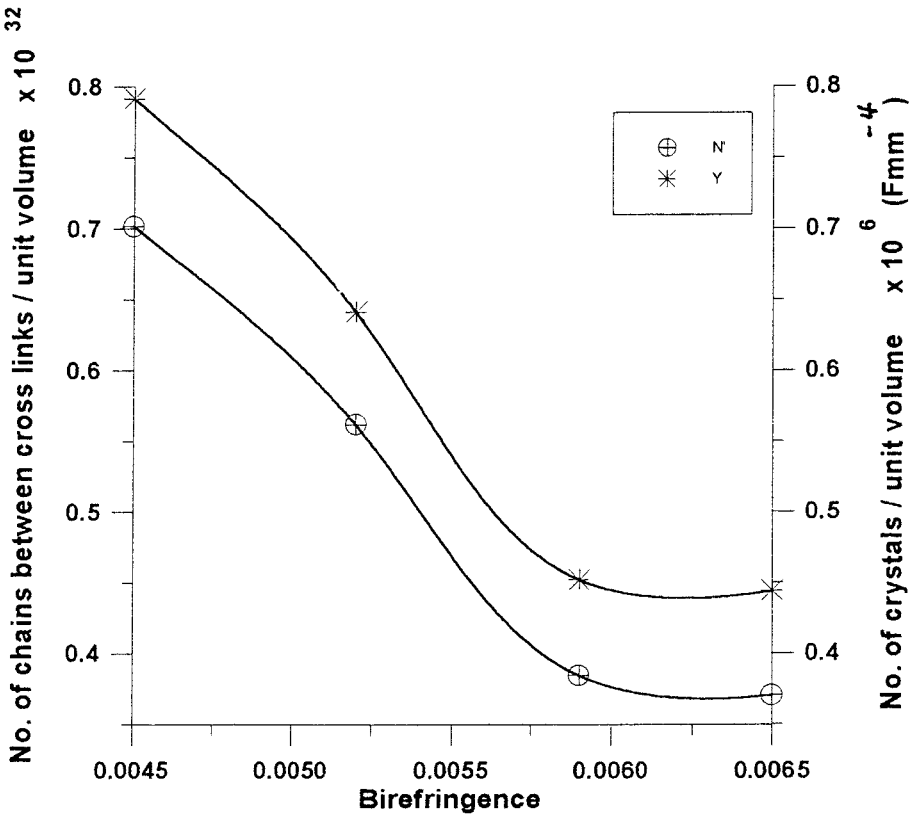

(b)

Figure 7 The N' and Y versus the (a) draw ratio and (b) birefringence.

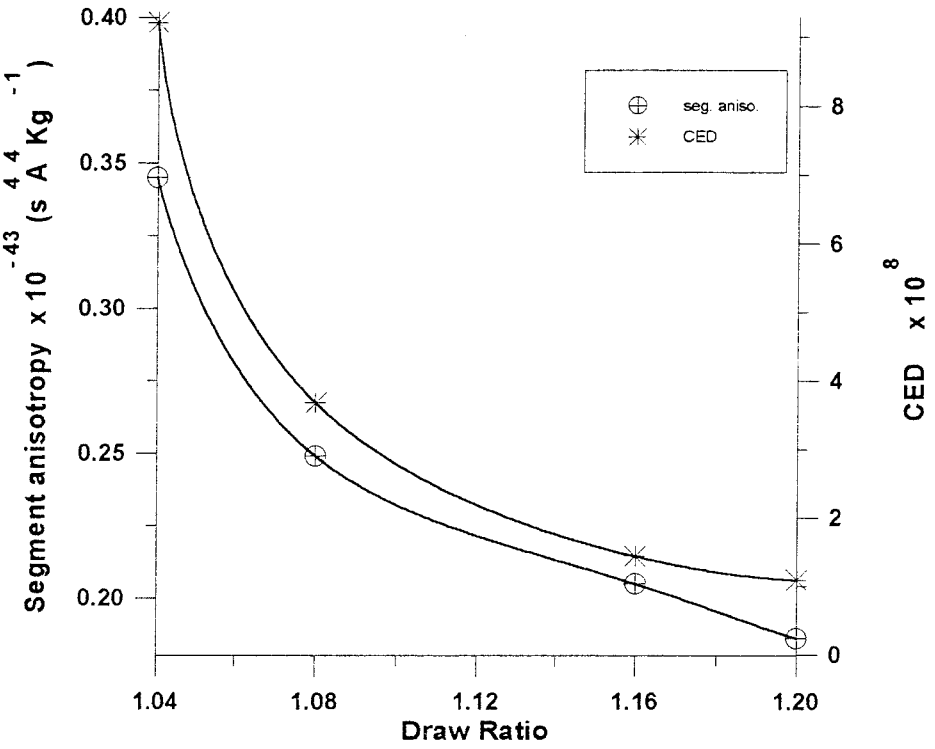

Figure 8 The segment anisotropy and cohesive energy density (CED) and their relationships with the draw ratio.

Application of stress makes the easily deformable phase gradually convert into the less deformable phase. On the release of stress, they recover their original dimensions with rebound. The shrinkage parameters are an indication for this observation.[31] The irregularity along the fiber axis in both the fiber diameter and fringe shift, as shown in Figure 3(a–c), arises from the necking of the viscose fiber during drawing. Thus, in the present study the optical parameters produced in fibers due to stretching gave valuable information for characterizing several important parameters for industrial use.

CONCLUSION

1. The shrinkage stress, uniaxial tension, and true stress increase with increasing draw ratio. The mechanical orientation factor is always comparatively small.
2. The number of moles in physical network chains between entanglements per unit volume decreases as the draw ratio increases.
3. The segment anisotropy, the number of chains between crosslinks per unit volume, and the number of crystals per unit volume decrease with increasing draw ratio and boiling time.
4. The optical and mechanical orientations are different techniques that are suitable for predicting molecular orientations in viscose fibers. Every technique has its own contribution, and both increase as the draw ratio increases. The interference and mechanical techniques are suitable for calculating many structural parameters with fair accuracy.
5. The CED decreases as the draw ratio increases, which could help in solving solubility problems.

REFERENCES

1. Statton, W. O. J Polym Sci Part C 1967, 20, 117.
2. Statton, W. O.; Koenig, J. L.; Hannon, M. J Appl Phys 1970, 41, 1069.
3. Jabarin, S. A. Polym Eng Sci 1984, 24, 376.
4. Sharma, S. K.; Misra, A. J Appl Polym Sci 1987, 34, 2231.

5. Ward, I. M. J Polym Sci Polym Symp 1977, 58, 1.
6. Bernhard, W. Macromolecular Physics, Volume 1: Crystal Structure, Morphology, Defects (A); London, 1973.
7. Barakat, N.; Hamza, A. A. Interferometry of Fibrous Materials; Hilger: London, 1990.
8. Hamza, A. A.; Fouda, I. M.; Kabeel, M. A.; Shabana, H. M. Polym Test 1996, 15, 301.
9. Fouda, I. M.; Shabana, H. M. Polym Int 1999, 48, 602.
10. Fouda, I. M.; Shabana, H. M. J Appl Polym Sci 1999, 72, 1185.
11. Shabana, H. M. Polym Polym Compos 1999, 7, 125.
12. Fouda, I. M.; Shabana, H. M. Eur Polym J 2000, 36, 823.
13. Fouda, I. M. Polym Polym Compos 1998, 6, 513.
14. Peterlin, A. J Mater Sci 1971, 6, 490.
15. Vinogradov, G. V.; Ozyara, E. A.; Malkin, A. Y.; Grcchanovskii, V. A. J Polym Sci 1971, A-2, 1153.
16. Stein, R. S. J Polym Sci 1959, 24, 709.
17. Hermans, P. H. Contributions to the Physics of Cellulose Fibers; North Holland: Amsterdam, 1949; Chap. 3.
18. Treloar, L. R. G. The Physics of Rubber Elasticity, 2nd ed.; Oxford University Press: London, 1958.
19. Gedde, U. F. W. Polymer Physics; Chapman & Hall: London, 1995; p 214.
20. Hermans, P. H.; Platzek, P. Kolloid Z 1939, 88, 67.
21. Born, M.; Wolf, E. Principles of Optics, 2nd ed.; Pergamon: London, 1964; p 88.
22. Klein, P. G.; Ladizesky, N. H.; Ward, I. M. J Polym Sci Part B Polym Phys 1986, 24, 1093.
23. Hemsley, D. A. Applied Polymer Light Microscopy; Elsevier Science Publishers Ltd.: London, 1989; p 193.
24. Jenkins, A. D. Polymer Science Hand Book 1; North Holland: Amsterdam, 1972; p 505.
25. Fouda, I. M.; Shabana, H. M. Polym Polym Compos 2000, 8, 51.
26. Pluta, M. Opt Acta 1971, 18, 661.
27. Ward, I. M. Proc Phys Soc 1962, 80, 1176.
28. (a) Mooney, M. J Appl Phys 1940, 11, 582; (b) Mooney, M. J Appl Phys 1948, 19, 434; (c) Rivlin, R. S. Trans R Soc (Lond) 1948, A241, 379; (d) Sperling L. H. Introduction to Physical Polymer Science, 2nd ed.; Wiley: New York, 1992.
29. Decandi, F.; Vittoria, V.; Peterlin, A. J Polym Sci Polym Phys Ed 1985, 23, 1217.
30. Fouda, I. M.; El-Tonsy, M. M.; Metawe, F. M.; Housny, H. H.; Eassawi, K. H. Polym Test 1998, 17, 461.
31. Ward I. M. J Polym Sci Polym Symp 1977, 53, 9.
32. Williams, D. J. Polymer Science and Engineering; Prentice–Hall: Englewood Cliffs, NJ, 1971; p 267.